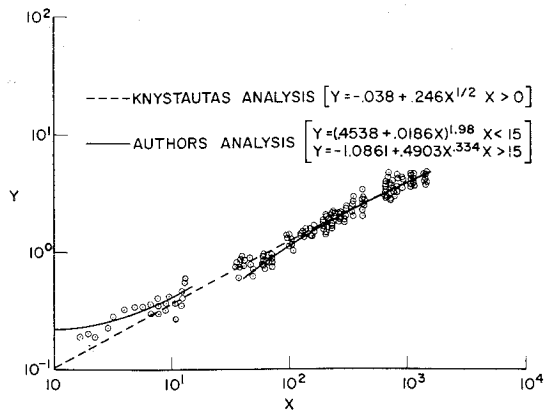

Fig. 3 Plot of authors' analysis of Knystautas data.

region which is appropriate for the M_∞ considered in this analysis.

The data were subjected to fitting to both Eqs. (1) and (2). In cases where $X < 15$, the highest correlation coefficients were obtained with Eq. (2). In the region of $X > 15$, Eq. (1) gave the best fit reflecting its development with data weighted toward the far wake.

Figure 2 is a plot of the equations shown in Table 1. The equations representing the near wake are concave upward and the far wake are concave downward indicating that at least one inflection point exists, even though it has not been explicitly located.

Figure 3 shows a plot of Knystautas[6] reduced data along with his fit to his data. The Knystautas[6] fit shown as the dashed line was done for all values of X. The authors' fitting of Knystautas[6] data for $X < 15$ and $X > 15$ are shown as the solid lines. The authors' fit of Knystautas[6] data for all values of X gave $N = 0.44$ which compares with the $N = 0.50$ he obtained.

Summary

The analysis of the authors' data alone indicated that the best data fit in the pressure expansion controlled region ($P_w > 4P_\infty$) and the mixed pressure expansion-thermal diffusion region ($4P_\infty > P_w > P_\infty$) gave a value of $N > 1.0$. The same analysis of other investigators' data in the same regions also revealed values of $N > 1.0$, whereas analysis of the same data for $P_w \approx P_\infty$ revealed values of $N < 1.0$. The selection of $X \approx 15$ as the dividing point where $P_w \approx P_\infty$ is based on Lees and Hromas[7] theoretical treatment of the wake and the M_∞ of the authors' data used in this analysis. The analysis shows that the rapid growth of the near wake expected by Lees and Hromas[7] does exist and is experimentally detectable. It is also apparent that analyses using data predominantly from the thermally controlled region of the far wake will result in a value of N approximating the $\frac{1}{3}$ law very closely. Because the thermally controlled region is by far the larger region, analyses including all values of X weighs the power dependence heavily toward the 0.33 power which is not suitable for values of X where $P_w \gg P_\infty$. Equation (2) seemed to fit the data better for $X < 15$ whereas the form of Eq. (1) fit better for $X > 15$. This analysis indicates that the 0.33 power law for the wake growth is applicable only in the purely thermal region and is not applicable for all values of X.

References

[1] Slattery, R. E. and Clay, W. G., "Width of the Turbulent Trail Behind a Hypervelocity Sphere," *The Physics of Fluids*, Vol. 4, 1961, pp. 1199–1201.

[2] Murphy, C. H. and Dickinson, E. R., "Growth of the Turbulent Wake behind a Supersonic Sphere," *AIAA Journal*, Vol. 1, No. 2, Feb. 1963, pp. 339–342.

[3] Wilson, L. N., "Far-Wake Behavior of Hypersonic Blunted Cones," *AIAA Journal*, Vol. 5, No. 8, Aug. 1967, pp. 1393–1396.

[4] Fay, J. A. and Goldburg, A., "The Unsteady Hypersonic Wake Behind Spheres," Paper 2676-62, Nov. 1962, ARS.

[5] Dana, T. A. and Short, W. W., "Experimental Studies of Hypersonic Turbulent Wakes," Rept. ZPH-103, 1961, General Dynamics/Convair.

[6] Knystautas, R., "The Growth of the Turbulent Inner Wake Behind a Three-Inch Diameter Sphere," TR 488, Jan. 1964, Canadian Armament Research and Development Establishment.

[7] Lees, L. and Hromas, L., "Turbulent Diffusion in the Wake of a Blunt-Nosed Body at Hypersonic Speeds," *Journal of the Aerospace Sciences*, Vol. 29, 1962, pp. 976–993.

Viscous Effects on the Flow Coefficient for a Supersonic Nozzle

P. F. Massier,* L. H. Back,† M. B. Noel,‡ and F. Saheli§

Jet Propulsion Laboratory, California Institute of Technology, Pasadena, Calif.

Nomenclature

A = area, in.^{2}
C = $[2/(\gamma + 1)]^{1/(\gamma-1)}[2g\gamma/R(\gamma + 1)]^{1/2}$
C_D = flow coefficient
D = diameter, in.
H_{t0} = stagnation enthalpy in reservoir
$\dot{m}$ = mass flow rate, lb/sec
M = Mach number
p = pressure, psia
r = radius, in.
$Re_{D_{th}}$ = throat Reynolds number, $(\rho_e u_e D/\mu_e)_{th}$
T = temperature, °R
u = velocity parallel to wall
x = distance along wall
y = distance normal to wall
β = acceleration parameter
γ = specific-heat ratio
δ = boundary-layer thickness
δ^* = displacement thickness
θ = momentum thickness
μ = viscosity
ν = kinematic viscosity
ξ = transformed coordinate along wall
ρ = density

Subscripts and superscripts

c = curvature at throat
e = edge of boundary layer
t = stagnation condition
th = throat condition
w = wall condition
$(\ )^*$ = sonic condition
$1-D$ = one-dimensional isentropic
$\overline{(\ )}$ = mean value

Introduction

EXPERIMENTAL values of adiabatic flow coefficient are presented for choked flow in a supersonic nozzle which had a contour as shown in Fig. 1. Throat Reynolds numbers ranged between 650 and 350,000. Previously, there have apparently been no such measurements available for choked

Received October 30, 1969. This work represents the results of one phase of research carried out in the Propulsion Research and Advanced Concepts Section of the Jet Propulsion Laboratory, California Institute of Technology, under Contract NAS 7-100, sponsored by NASA.

* Group Supervisor.
† Member of Technical Staff.
‡ Senior Engineer.
§ Graduate Student, Colorado State University, Fort Collins, Colo.

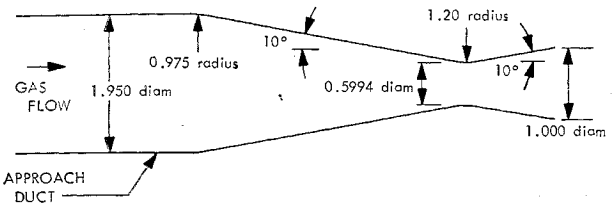

Fig. 1 Nozzle configuration (all dimensions in inches).

nozzle flow over the major portion of this Reynolds number range; for example, see Refs. 1 and 2 for measurements at throat Reynolds numbers below about 200 and above about 400,000, respectively. The adiabatic flow coefficient is influenced by the nozzle contour, particularly in the throat region which establishes the inviscid core flow distribution, and by the viscous (boundary-layer) effects. In the experiments, which were conducted with argon, nitrogen, and helium, the boundary layers in the throat region of the nozzle are believed to have been laminar even at the higher throat Reynolds numbers because of the high values of the acceleration parameter $K = (\nu_e/u_e^2)(du_e/dx)$. With this nozzle, viscous effects could be investigated directly because for a value of the ratio of throat radius of curvature to throat radius of 4, the inviscid flowfield does not differ much from that for one-dimensional flow, as indicated by a predicted value of $C_{D\text{inv}} = 0.998$ for $\gamma = 1.67$ (see Refs. 3 and 4).

Experimental Apparatus

The flow coefficient is defined as the ratio of the actual mass flow rate to the theoretical mass flow rate for a one-dimensional isentropic expansion from a reservoir condition to sonic velocity at the throat of the nozzle. Experimental flow coefficients were evaluated, using the following equation:

$$C_D \equiv \frac{\dot{m}}{\dot{m}_{1-D}} = \frac{1}{C}\left[\frac{\dot{m}(T_t)^{1/2}}{p_{\text{th}}A_{\text{th}}}\right] \tag{1}$$

The values of C used were 0.662 for argon, 0.523 for nitrogen, and 0.2098 for helium. The actual mass flow rate $\dot{m}$ was measured with a rotameter that had been carefully calibrated with each of the gases used, at about the same temperature and pressure in the rotameter as existed during the experiments so that corrections for pressure and temperature were kept small. Calibration of a given rotameter reading was accomplished by means of a balance and known weights to determine the quantity of gas that was discharged from pressurized containers during a measured time interval. The scatter of the calibration data at any given rotameter reading did not exceed $\pm 0.3\%$ of the average measurement at that reading. The stagnation temperature of the gas was near room temperature. The stagnation pressure near the nozzle inlet in the approach duct was computed by adding the dynamic pressure to the wall static pressure which was measured with a manometer containing oil. For all of the low and most of the high Reynolds number tests, this manometer was referenced to an evacuated chamber in which the absolute pressure was measured with a Kinney gage and was never above 0.050 mm Hg. For the other tests, the ambient pressure was used as reference which was measured with a barometer. The throat diameter of the nozzle (0.5994 in.) was measured with an internal tri-point micrometer to an estimated accuracy of ± 0.0002 in.

The length of the approach duct was about 4 diam for the nitrogen, helium, and some of the argon tests, and about 8 diam for the other argon tests. An effect of upstream length on C_D could not be detected. The Mach number in the approach duct was 0.05. The nozzle exit was connected to a vacuum system; thus, data could be obtained at stagnation pressures below one atmosphere; the range investigated was between 0.04 and 20 psia.

Experimental Results and Predictions

The experimental results, shown in Fig. 2, indicate that the flow coefficient ranged from about 0.94 at the smallest Reynolds number to about 0.98 at the largest Reynolds number. Data obtained from all three gases produced consistent results, although tests at the low Reynolds numbers were conducted only with argon. A continuously decreasing flow coefficient is expected as the Reynolds number is reduced because the boundary layer extends farther across the throat and, hence, proportionately more of the mass flows through the viscous layer. The line shown in Fig. 2 is a prediction to be discussed subsequently, based on laminar boundary-layer flow.

Since the flow is essentially parallel to the centerline in the throat plane, the influence of the viscous effect on C_D may be shown as follows:

$$C_D \equiv \frac{\dot{m}}{\dot{m}_{1-D}} = \frac{\int_0^{r_{\text{th}}} \rho u(2\pi r)dr}{\rho^* u^*(\pi r_{\text{th}}^2)}$$

This expression can be rearranged in the following form:

$$C_D = \frac{\int_0^{r_{\text{th}}} (\rho u)_{\text{inv}}(2\pi r)dr}{(\rho u)^*(\pi r_{\text{th}}^2)} - \frac{1}{(\rho u)^*(\pi r_{\text{th}}^2)} \int_{r_{\text{th}}-\delta}^{r_{\text{th}}} [(\rho u)_{\text{inv}} - \rho u](2\pi r)dr$$

The first term is recognized as the flow coefficient for an inviscid flow. From the definition of the boundary-layer displacement thickness δ^*,

$$\int_{\delta^*}^{\delta} (\rho u)_{\text{inv}}(2\pi r)dy = \int_0^{\delta} \rho u(2\pi r)dy$$

The second term can be rewritten to give the flow coefficient as

$$C_D = C_{D\text{inv}} - 2\left[\frac{(\overline{\rho u})_{\text{inv}}}{(\rho u)^*}\right]\frac{\delta^*}{r_{\text{th}}}\left(1 - \frac{\delta^*}{2r_{\text{th}}}\right)$$

where $(\overline{\rho u})_{\text{inv}}$ is the average value across the displacement thickness. Since the quantity $[(\overline{\rho u})_{\text{inv}}/(\overline{\rho u})^*]$ is only slightly less than unity and the term $(\delta^*/2r_{\text{th}})$ is small compared to unity for the flow considered herein, a good approximation for the flow coefficient that explicitly indicates the inviscid and viscous effects¶ is given by

$$C_D \cong C_{D\text{inv}} - 2(\delta^*/r_{\text{th}}) \tag{2}$$

Equation (2) was used to predict the flow coefficient by making an estimate of the displacement thickness for laminar boundary-layer flow, using the prediction method of Cohen and Reshotko[5] which is based upon the solution of the integral form of the momentum equation. In the prediction, the laminar boundary layer was assumed to originate at the inlet of the 4-diam long tube preceding the nozzle. The freestream flow variables were determined from wall static-pressure measurements made along the nozzle for argon flow. Although the throat Reynolds numbers and, consequently, the Reynolds numbers per unit length became fairly large at the higher stagnation pressures, it is doubtful that transition from a laminar to a turbulent boundary layer occurred along the tube. In the tube, the largest length Reynolds number based on the distance from the tube inlet to the nozzle inlet was 3.6×10^5. However, if transition to a turbulent boundary layer did occur in the tube at the higher Reynolds numbers, the boundary layer probably would not have remained turbulent through the convergent section of the nozzle because of the effect of acceleration on the structure of a turbulent boundary layer. Turbulent boundary layers

¶ A similar derivation for two-dimensional flow through a nozzle with a rectangular cross section gives $C_D \cong C_{D\text{inv}} - (\delta^*/h_{\text{th}})$; where h_{th} is the throat half-height.

Table 1 Effect of cooling on the displacement thickness for a compressible laminar boundary-layer flow over a cooled, isothermal wall, Prandtl number of unity, viscosity proportional to temperature, and constant specific heat; sonic condition $M_e = 1$, acceleration parameter $\beta = (2\xi/M_e)(dM_e/d\xi) = 20$, flow-speed parameter $(u_e^2/2H_{t0}) = \frac{1}{4}$ or $\gamma = \frac{5}{3}$ (Ref. 7)

Parameters	Units				
(T_w/T_t)	0	0.2	0.6	0.8	1.0
(δ^*/θ)	−0.84	−0.61	0.19	1.05	3.11

have been found to undergo reverse transition toward a laminar boundary layer when values of the parameter $K = (\nu_e/u_e^2)(du_e/dx)$ exceed about 2×10^{-6}. The parameter K, which is inversely proportional to the Reynolds number for nozzle flow, exceeded this value through the convergent section of the nozzle even at the highest throat Reynolds number. Recent boundary-layer measurements[6] in a similar nozzle with a 10° half-angle of convergence indicated laminarization of an originally turbulent boundary layer to occur for values of the throat Reynolds number as large as 6.5×10^5. At the lowest throat Reynolds number, the predicted ratio of momentum thickness to throat radius at the throat was 0.010, and the predicted ratio of displacement thickness to momentum thickness δ^*/θ was 3.4. With increasing throat Reynolds number, the ratio (θ/r_{th}) decreases since, for laminar boundary layers, $(\theta/r_{th}) \propto 1/(Re_{D_{th}})^{1/2}$. As seen in Fig. 2, the predicted curve passes through the data at the small Reynolds numbers and lies slightly above the data at the large Reynolds numbers.

Wall Cooling Effect

An interesting aspect of the relation given by Eq. (2) is that the flow coefficient may exceed unity under certain conditions, namely, if the mass flux through the boundary layer exceeds the mass flux in the inviscid flow by a sufficient amount to offset the contribution of $C_{D_{inv}}$, a value always less than unity. For this situation the displacement thickness is negative, i.e., the effective boundary-layer displacement is no longer outward from the throat surface, but inward. Wall cooling can lead to negative displacement thicknesses as indicated in Table 1, where predicted values of (δ^*/θ) are shown from some exact solutions[7] of the compressible laminar boundary-layer equations for a typical condition at a nozzle throat. These local similarity solutions indicate negative displacement thicknesses, for values of the wall to stagnation temperature ratio (T_w/T_t), of less than about 0.5.

Summary and Conclusions

Experiments to determine the adiabatic flow coefficient in a supersonic nozzle with choked flow conducted over a throat Reynolds number range between 650 and 350,000 indicated that C_D varied continuously between 0.94 at the smallest Reynolds number and 0.98 at the largest Reynolds number. This trend of an increasing flow coefficient with Reynolds number is in agreement with a laminar boundary-layer prediction, although most of the data points at the intermediate and higher Reynolds numbers were somewhat lower than the predicted values of C_D.

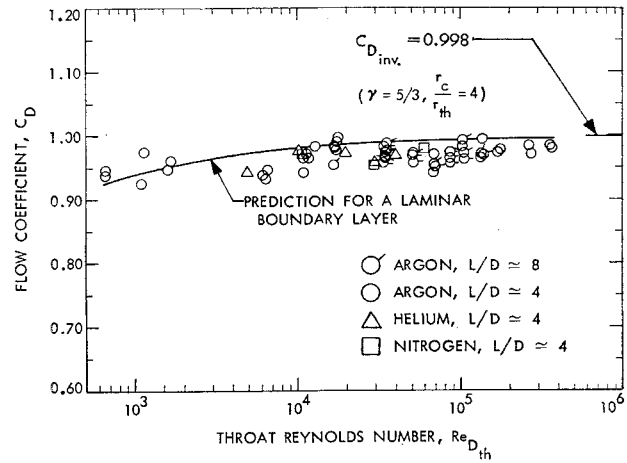

Fig. 2 Variation of the flow coefficient with Reynolds number for ambient temperature and a stagnation pressure range from 0.04 to 20 psia.

References

[1] Sutherland, G. S. and Maes, M. E., "A Review of Microrocket Technology: 10^{-6} to 1 lbf Thrust," *Journal of Spacecraft and Rockets*, Vol. 3, No. 8, Aug. 1966, pp. 1153–1165.

[2] Back, L. H., Massier, P. F., and Gier, H. L., "Comparison of Measured and Predicted Flows Through Conical Supersonic Nozzles, with Emphasis on the Transonic Region," *AIAA Journal*, Vol. 3, No. 9, Sept. 1965, pp. 1606–1614.

[3] Sauer, R., "General Characteristics of the Flow through Nozzles at Near Critical Speeds," TM-1147, June 1947, NACA.

[4] Oswatitsch, K. and Rothstein, W., "Flow Pattern in a Converging-Diverging Nozzle," TM-1215, March 1949, NACA.

[5] Cohen, C. B. and Reshotko, E., "The Compressible Laminar Boundary Layer with Heat Transfer and Arbitrary Pressure Gradient," R-1294, 1956, NACA; supersedes TN-3326, 1955, NACA.

[6] Back, L. H., Cuffel, R. F., and Massier, P. F., "Laminarization of a Turbulent Boundary Layer in Nozzle Flow," *AIAA Journal*, Vol. 4, No. 4, April 1969, pp. 730–733.

[7] Back, L. H., "Acceleration and Cooling Effects in Laminar Boundary Layers—Subsonic, Transonic, and Supersonic Speeds," *AIAA Journal*, to be published.